International Journal of Power Electronics and Drive Systems (IJPEDS)
Vol. 14, No. 4, December 2023, pp. 2240~2253
ISSN: 2088-8694, DOI: 10.11591/ijpeds.v14.i4.pp2240-2253

Grid power control of direct matrix converter fed three-phase induction generator

Ali Salam Al-Khayyat[1], Human Qahtan Kadhem[2], Mustafa Jameel Hameed[1]
[1]Department of Electrical and Electronics Engineering, Faculty of Engineering, University of Thi-Qar, Nasiriyah, Iraq
[2]Electrical Power Techniques Engineering, Basrah Technical College, Southern Technical University, Basrah, Iraq

Article Info

Article history:

Received Apr 12, 2023
Revised Jun 8, 2023
Accepted Jun 25, 2023

Keywords:

Bidirectional switch
Direct matrix converter
Power electronic converters
Space vector modulation SVM
Power control

ABSTRACT

The direct matrix converter (DMC) and the modulation technique were presented in this paper, moreover the power of the grid is controlled. Due to its high flexibility and low computation demands, the DMC's most widely used modulation technique is space vector modulation. The double-side modulation is used in this paper instead of the single-side modulation because less harmonics at the input and output side can be obtained, however this would increase slightly the number of branch-switch-overs (BSO) for each switching period. In addition to being able to create input and output sinusoidal currents with various frequencies, it would adjust the input power factor. Along with that, the simple power control loop would regulate the grid power and then generate controlled three-phase reference signals for pulses generation accordingly. Results from the simulations show that the topology is appropriate for machine drive applications.

Corresponding Author:

Ali Salam Al-Khayyat
Department of Electrical and Electronics Engineering, Faculty of Engineering, University of Thi-Qar
Nasiriyah, Iraq
Email: ali-al-khayyat@utq.edu.iq

1. INTRODUCTION

In the world of power electronics, matrix converters (MCs) rank among the most desirable converter families. The matrix converter, which is also known as the “all-silicon” solution, is an array of controlled bidirectional semiconductor switches that directly connects the input voltage source to a load/output without using a DC-link stage or any other sort of energy storage device. By conducted research of Venturini and Alesina, this converter's development began in 1980. They presented the circuit configuration together with a comprehensive mathematical model to explain the converter's low-frequency behavior. They were the first who used the term “matrix converter”. This converter offers a few appealing qualities, which are:

- High power density
- Frequency decoupling of the AC input and output voltage
- Input and output Sinusoidal currents waveform
- Fully operating in regenerative mode
- Per required input power factor adjustment

Due to their ability to provide a small-footprint solution for a frequency converter, matrix converters are the subject of intense study at the moment. When compared to analogous two-stage power conversion methods, the MC can produce higher power densities. As a result, given the matrix converter's benefits of energy savings and size reduction, it is anticipated that its application areas will grow. Uninterruptible power supply (UPS), power factor correction (PFC) rectifiers for data centers and telecommunications equipment, battery energy storage systems (BESS), and a number of isolated AC-DC matrix converters have recently been proposed. The matrix converter, that is known as the direct matrix converter (DMC), has been subject to many modulation techniques since the 1980s. As a result, the DMC will be used in this work. Figure 1 depicts the primary force-commutated three-phase AC-AC converters' layout, which is called the DMC [1]–[3].

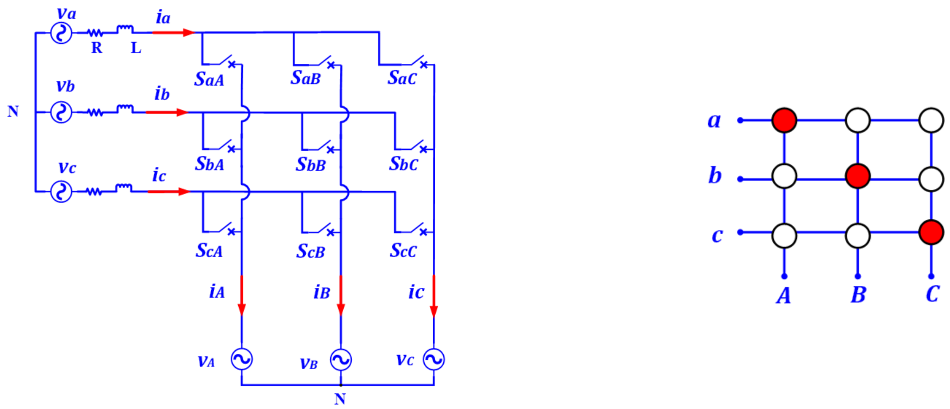

(a) (b)

Figure 1. Topology of a direct matrix converter (a) circuit diagram and (b) symbol of switching operation

The MC topology considers as one of the most researched converters, but it is not exploit in the industry. The restriction of input/output voltage transfer ration for sinusoidal modulation that is 86% maximum and the limitation of compensate the reactive power, make the MC not to compete with the conventional voltage source converter (VSC). Other issues need to be addressed in order to make the MC as a converter in the power electronic market are the lack of monolithic bidirectional semiconductors and the necessity of complex strategies for the commutation of the bidirectional power switches, which typically necessitates a control system based on FPGA [4], [5].

In this paper, the following is achieved:

– The direct space vector modulation matrix converter is implemented with double-side modulation due to less harmonics.
– The grid power will be controlled by employing simple power control loop that would provide the required frequency of the reference signal for generation the pulses. This is simplest approach of controlling the power without adding complexity to the modulation system, hence it will reduce the burden when the system is implemented experimentally.

2. DIRECT MATRIX CONVERTER

Direct matrix converter is a designed single-stage that links an m-phase voltage source to an n-phase load using a set of m×n bidirectional power switches. The (3-3) phase matrix converter considered as significant topology, because it connects the grid or any input voltage source to any three-phase output, such as motor. The power circuit of MC consists of nine bidirectional switches, which are arranged in a group of three, each group contains three switches. Additionally, each group may be referred to as a switching cell (SwC). As shown in Figure 1(a), this configuration enables the connection of any of the input phases (a, b, or c) to any of the output phases (A, B, or C). The schematic is arranged like a matrix, with the three output phases (A, B, and C) forming the columns and the three input phases (a, b, and c) forming the rows. Figure 1(b) circles represent the bidirectional switches that connect the rows and columns [1]–[3], [6]–[9].

The concept of the switching function can be used in a mathematical equation to represent the matrix converter operation, where an input phase j is connected to output phase K and is modeled by the switching function, S_{jk}. The switching function produces a result of 1 when the device is closed and a result of 0 when the device is open. Therefore, the following is the definition of a single device's switching function as (1):

$$S_{jk} = \begin{cases} 1, & S_{jk}\ Closed \\ 0, & S_{jk}\ Open \end{cases} \quad j = \{a, b, c\},\ k = \{A, B, C\} \tag{1}$$

2.1. Potential switching states

In MC, there is no freewheeling path that is exist in the conventional VSCs. That would make the safe transition between the permitted state of switching cells, more difficult. In order to satisfy the restriction of Eq.8, the bidirectional switches commutation should be happened instantly and simultaneously. This is not practicable, though, because of propagation delays in command circuits and limited switching times for power semiconductors [3], [7], [10]–[15].

There are two key guidelines for safe switching between switches in a switching cell:

- To avoid a short circuit of the sources of the input voltage, it is necessary to avoid connecting two devices at once to the same output line.
- One device needs to be conducting at all times in order to create a path for the current of the inductive load and avoid over-voltages.

Phase-to-Phase short circuits or over-voltages could harm the converter if these rules are not followed. These restrictions can be as (2):

$$S_{aK} + S_{bK} + S_{cK} = 1\ , K = \{A, B, C\} \tag{2}$$

The $3\ phase - 3\ phase$ matrix converter looks to have 29 distinct switch combinations, but with these restrictions, there are only 27 permitted switching states. The allowable switch states, which are separated into three groups, are summarized in Figure 2. The three-letter code that identifies which input line the corresponding output phase is attached to for each of these switch combinations gives it a unique look (see Figure 1(b)). As an illustration, the symbol "abb" indicates that the input lines a, b, and b are each connected to one of the output phases, A, B, or C. One space vector for output voltage and one input current are specified for each switching state of the matrix converter. Voltage (current) switching space vectors (SSV) are another name for these vectors. As a result, the MCs combine the input voltages to create the output voltage (input current) vector (output currents). The 27 permitted switching states are grouped into three categories based on the traits of the SSV connected to each switching state, as illustrated in Figure 2.

- Six switching states in Group I create a path between various input and output phases. The amplitudes of these SSV are constant. SSV for current and voltage rotates at the output frequency ω_0 and ω_i, respectively.
- Group II consists of 18 switching states in which two phases of output are connected to one input phase, while the third phase of the output is coupled to a different input phase. The fixed directions of these voltage/current SSVs are uniformly 60°apart in the αβ frame. These SSVs are referred to as “stationary vectors” for this reason. The magnitude of these voltage/current SSVs is dependent on the phase angles of the input voltage and output current, respectively. The output voltage vectors' magnitude can reach $(2/\sqrt{3})\ V_{env}$, where V_{env} represents the current state of the rectified input voltage envelope.
- Group III consists of three configurations in which the same input phase is coupled to all three output phases. Since the vectors of output voltage and input current from these SSVs are zero (i.e., at the $\alpha\beta$ frame's origin), they will be referred to as “zero vectors” [2], [3], [7], [9]–[11], [14], [16], [17].

2.2. Modulation of direct matrix converter

The SVM representation of the input current and output voltage in the “Park” frame serves as the foundation for the space vector approach. 27 variants are viable for the direct matrix converter's three-phase construction. Compared to other techniques, the SVM has advantages which are:

- Prompt commutation perception
- Highest possible voltage transfer ratio without the use of third harmonics injection is achieved
- The power factor of the input and output can be controlled separately
- Reduce the switching losses by minimizing the number of times each cycle needs to switch
- As little harmonic content as possible and simple digital implementation

The representation of instantaneous space vector of the input and output currents and voltages on the $\alpha\beta$ reference frame serves as the basis for space vector modulation. The space vector for the immediate output voltage, the instantaneous input current space vector, and the voltage space vector of the input as (3):

$$\begin{aligned}
\overline{v_0} &= \frac{2}{3}(v_{AB} + a\ v_{BC} + a^2\ v_{CA}) = v_o\ e^{j\alpha_0} \\
\overline{\iota_i} &= \frac{2}{3}(i_a + a\ i_b + a^2\ i_c) = i_i\ e^{j\beta_i} \\
\overline{v_i} &= \frac{2}{3}(v_a + a\ v_b + a^2\ v_c) = v_i\ e^{j\alpha_i}
\end{aligned} \tag{3}$$

Where $a = e^{j\frac{2\pi}{3}}$, v_o, and α_0 are the magnitude and angle of $\overline{v_0}$. i_o and β_i are the magnitude and angle of $\overline{\iota_\iota}$. v_i and α_i are the magnitude and angle of $\overline{v_\iota}$. Group I's output voltage and input current SSVs rotate in the $\alpha\beta$ frame, making it impossible to utilize them to successfully reconstruct the reference vectors. Because of this, in an SVM method, only the stationary and zero vectors are used. The switching configurations of the $3\,phase - 3\,phase$ matrix converter utilized in direct SVM are listed in Table 1. Figures 3(a) and 3(b) illustrate the representation of output voltage and input current SSVs in the αβ frame. The spaces between each pair of neighboring SSVs are represented by sectors, which range from 1 to 6.

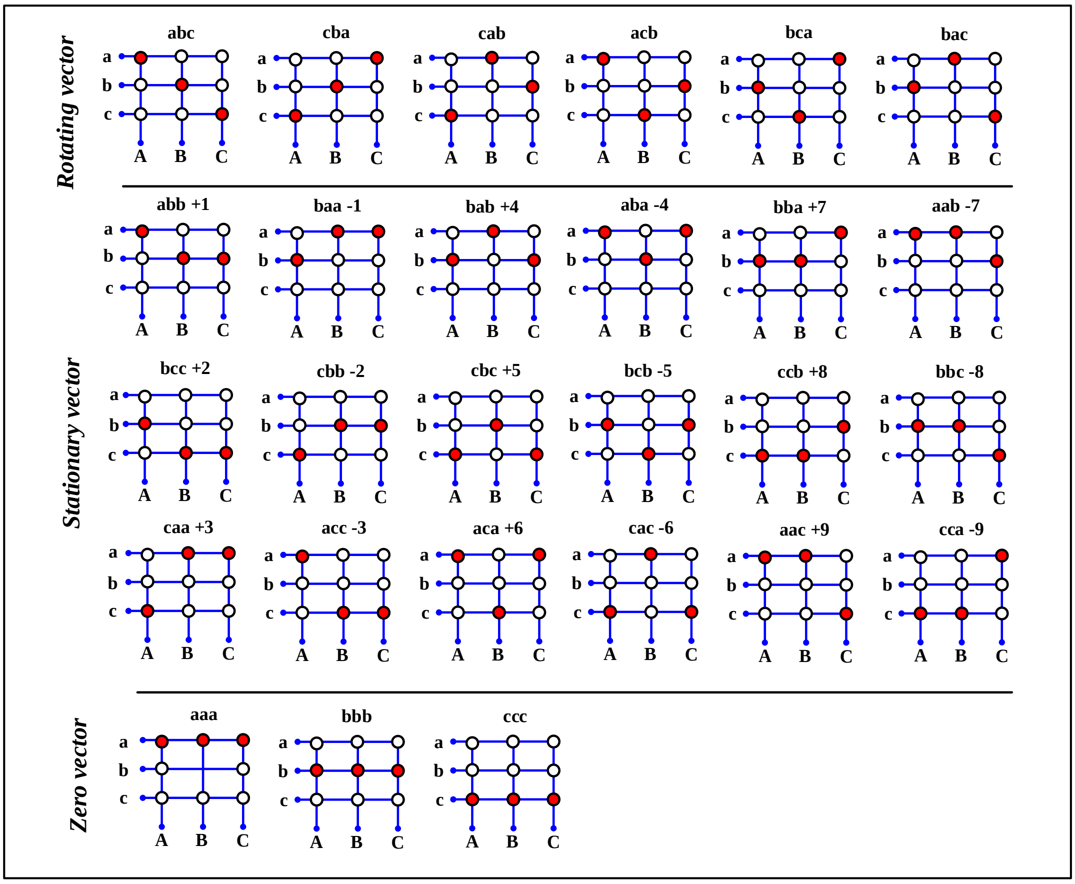

Figure 2. A matrix converter's 27 permitted switch states

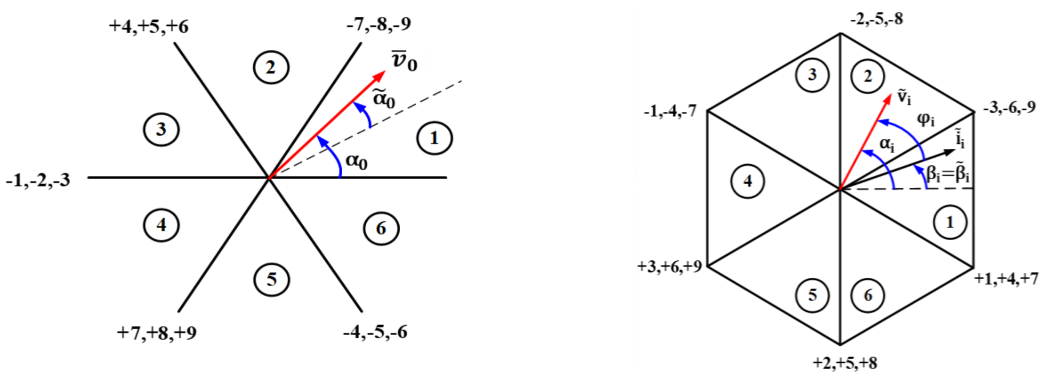

(a) (b)

Figure 3. Representation of stationary vectors in an $\alpha\beta$ frame: (a) switching state vector for output voltage and (b) switching state vector for input current

Table 1. Direct space vector modulation uses switching configurations for 3 Phase-3 Phase MC (SVM)

Switching Configuration	A	B	C	v_{AB}	v_{BC}	v_{CA}	i_a	i_b	i_c	v_0	α_0	i_i	β_i
+1	a	b	b	v_{ab}	0	$-v_{ab}$	i_A	$-i_A$	0	$(2/\sqrt{3})v_{ab}$	0	$(2/\sqrt{3})i_A$	$-\pi/6$
-1	b	a	a	$-v_{ab}$	0	v_{ab}	$-i_A$	i_A	0	$-(2/\sqrt{3})v_{ab}$	0	$-(2/\sqrt{3})i_A$	$-\pi/6$
+2	b	c	c	v_{bc}	0	$-v_{bc}$	0	i_A	$-i_A$	$(2/\sqrt{3})v_{bc}$	0	$(2/\sqrt{3})i_A$	$\pi/2$
-2	c	b	b	$-v_{bc}$	0	v_{bc}	0	$-i_A$	i_A	$-(2/\sqrt{3})v_{bc}$	0	$-(2/\sqrt{3})i_A$	$\pi/2$
+3	c	a	a	v_{ca}	0	$-v_{ca}$	$-i_A$	0	i_A	$(2/\sqrt{3})v_{ca}$	0	$(2/\sqrt{3})i_A$	$7\pi/6$
-3	a	c	c	$-v_{ca}$	0	v_{ca}	i_A	0	$-i_A$	$-(2/\sqrt{3})v_{ca}$	0	$-(2/\sqrt{3})i_A$	$7\pi/6$
+4	b	a	b	$-v_{ab}$	v_{ab}	0	i_B	$-i_B$	0	$(2/\sqrt{3})v_{ab}$	$2\pi/3$	$(2/\sqrt{3})i_B$	$-\pi/6$
-4	a	b	a	v_{ab}	$-v_{ab}$	0	$-i_B$	i_B	0	$-(2/\sqrt{3})v_{ab}$	$2\pi/3$	$-(2/\sqrt{3})i_B$	$-\pi/6$
+5	c	b	c	$-v_{bc}$	v_{bc}	0	0	i_B	$-i_B$	$(2/\sqrt{3})v_{bc}$	$2\pi/3$	$(2/\sqrt{3})i_B$	$\pi/2$
-5	b	c	b	v_{bc}	$-v_{bc}$	0	0	$-i_B$	i_B	$-(2/\sqrt{3})v_{bc}$	$2\pi/3$	$-(2/\sqrt{3})i_B$	$\pi/2$
+6	a	c	a	$-v_{ca}$	v_{ca}	0	$-i_B$	0	i_B	$(2/\sqrt{3})v_{ca}$	$2\pi/3$	$(2/\sqrt{3})i_B$	$7\pi/6$
-6	c	a	c	v_{ca}	$-v_{ca}$	0	i_B	0	$-i_B$	$-(2/\sqrt{3})v_{ca}$	$2\pi/3$	$-(2/\sqrt{3})i_B$	$7\pi/6$
+7	b	b	a	0	$-v_{ab}$	v_{ab}	i_C	$-i_C$	0	$(2/\sqrt{3})v_{ab}$	$4\pi/3$	$(2/\sqrt{3})i_C$	$-\pi/6$
-7	a	a	b	0	v_{ab}	$-v_{ab}$	$-i_C$	i_C	0	$-(2/\sqrt{3})v_{ab}$	$4\pi/3$	$-(2/\sqrt{3})i_C$	$-\pi/6$
+8	c	c	b	0	$-v_{bc}$	v_{bc}	0	i_C	$-i_C$	$(2/\sqrt{3})v_{bc}$	$4\pi/3$	$(2/\sqrt{3})i_C$	$\pi/2$
-8	b	b	c	0	v_{bc}	$-v_{bc}$	0	$-i_C$	i_C	$-(2/\sqrt{3})v_{bc}$	$4\pi/3$	$-(2/\sqrt{3})i_C$	$\pi/2$
+9	a	a	c	0	$-v_{ca}$	v_{ca}	$-i_C$	0	i_C	$(2/\sqrt{3})v_{ca}$	$4\pi/3$	$(2/\sqrt{3})i_C$	$7\pi/6$
-9	c	c	a	0	v_{ca}	$-v_{ca}$	i_C	0	$-i_C$	$-(2/\sqrt{3})v_{ca}$	$4\pi/3$	$-(2/\sqrt{3})i_C$	$7\pi/6$
0_a	b	a	a	0	0	0	0	0	0	0	-	0	-
0_b	a	b	b	0	0	0	0	0	0	0	-	0	-
0_c	c	c	c	0	0	0	0	0	0	0	-	0	-

2.3. Synthesis of vectors

The reference quantities $\overline{v_i}$ and φ_i are completely under the control of the SVM modulation by default. Let's use Figures 4(a) and 4(b) to illustrate how modulation works. The supply voltage controls $\overline{v_i}$, and measurement of its angle α_i is possible. By lining up vector $\overline{i_i}$ with $\overline{v_i}$, it would acquire unity power factor. By selecting four stationary vectors and applying them at appropriate intervals over the period T_s, the SVM modulation is accomplished.

It is assumed that $\overline{v_0}$ and $\overline{i_i}$ are both located in sector 1. The components of $\overline{v_0}$ together with the two SSVs are shown in Figure 4(a) as $\overline{v_0}^1$ and $\overline{v_0}^2$. Along with the existing SSVs, $\overline{i_i}$ in Figure 4(b) is similarly divided into $\overline{i_i}^1$ and $\overline{i_i}^2$. The switching configurations that can synthesize the elements of $\overline{v_0}$ and $\overline{i_i}$ are as (4) and (5):

$$\overline{v_0}^1 : \pm 7, \pm 8, \pm 9;$$

$$\overline{v_0}^2 : \pm 1, \pm 2, \pm 3; \tag{4}$$

$$\overline{i_i}^1 : \pm 3, \pm 6, \pm 9;$$

$$\overline{i_i}^2 : \pm 1, \pm 4, \pm 7; \tag{5}$$

Utilizing the common switching states $\pm 7, \pm 8, \pm 9$, and ± 3, we can simultaneously generate $\overline{v_0}$ and $\overline{i_i}$. Only one switching configuration having the same number and the reverse signs is used. They choose the ones with greater voltage values. These guidelines can be used to identify the four switching configurations for each combination of the output voltage sector (K_v) and the input current sector (K_i). Then, throughout the switching sequence, the four stationary vectors are time-averaged to create $\overline{v_0}$ and $\overline{i_i}$. As was already mentioned, the stationary vectors are applied using the appropriate duty cycles to generate both $\overline{v_0}$ and $\overline{i_i}$. They are calculated as follows using the phase of the input current vector reference $(\widetilde{\beta_i})$ and the phase of the output voltage vector reference $(\widetilde{\alpha_0})$ as (6)-(9):

$$\tau_1 = \frac{2}{\sqrt{3}}\, q \frac{cos(\widetilde{\alpha_0} - \frac{\pi}{3})\, cos(\widetilde{\beta_i} - \frac{\pi}{3})}{cos(\varphi_i)} \tag{6}$$

$$\tau_2 = \frac{2}{\sqrt{3}}\, q \frac{cos(\widetilde{\alpha_0} - \frac{\pi}{3})\, cos(\widetilde{\beta_i} + \frac{\pi}{3})}{cos(\varphi_i)} \tag{7}$$

$$\tau_3 = \frac{2}{\sqrt{3}}\, q \frac{\cos(\widetilde{\alpha_0}+\frac{\pi}{3})\cos(\widetilde{\beta_\iota}-\frac{\pi}{3})}{\cos(\varphi_i)} \tag{8}$$

$$\tau_4 = \frac{2}{\sqrt{3}}\, q \frac{\cos(\widetilde{\alpha_0}+\frac{\pi}{3})\cos(\widetilde{\beta_\iota}+\frac{\pi}{3})}{\cos(\varphi_i)} \tag{9}$$

Where the voltage transfer ratio is given by $q = |\overline{v_0}|/(\sqrt{3}|\overline{v_\iota}|)$. As seen in Figure 3, the angles utilized in (6)-(9) with regard to the sector's bisecting line were calculated. The output voltage and input current sectors are where they diverge from α_0 and β_i. The following are the limitations for $\widetilde{\alpha_0}$ and $\widetilde{\beta_\iota}$.

$$-\frac{\pi}{6} < \widetilde{\alpha_0} < +\frac{\pi}{6}$$

$$-\frac{\pi}{6} < \widetilde{\beta_\iota} < +\frac{\pi}{6} \tag{10}$$

The zero-vector duty cycle, τ_{a0}, τ_{b0}, and τ_{c0} are calculated at fixed sample in order to complete the period of switching, this is shown as (11):

$$\tau_{a0} + \tau_{b0} + \tau_{c0} = 1 - (\tau_1 + \tau_2 + \tau_3 + \tau_4) \tag{11}$$

As a result, the following restrictions are placed on the switching arrangements duty cycles as (12):

$$\tau_{a0}, \tau_{b0}, \tau_{c0} \geq 0$$

$$\tau_1, \tau_2, \tau_3, \tau_4 \geq 0 \tag{12}$$

By assuming that input and output voltages are balanced and considering in (6)-(12), hence the maximum transfer ratio of the voltage is given by (13):

$$q < \frac{\sqrt{3}}{2}|\cos\varphi_i| \tag{13}$$

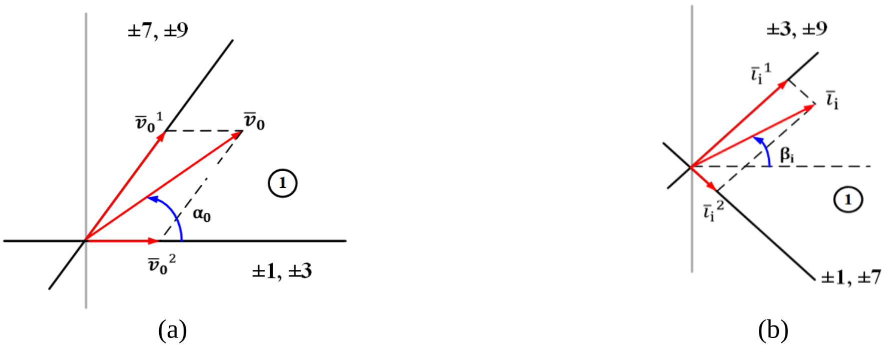

Figure 4. Modulation concept (a) $\overline{v_0}$ and (b) $\overline{\iota_\iota}$

3. THE APPROACH OF POWER CONTROL

In this paper, the power of the grid would be regulated and simple control is used. Where the three-phase reference signal for generation the pulses is achieved. The active power of the Induction Generator IG is calculated then it is compared with the desired active power and the error is processed by PI controller, which would generate the frequency. This frequency is used to generate the three-phase reference signal for pulse generation. The power control structure is shown in Figure 5, and the generation of reference signal for pulses generation.

3.1. Controlled three phase generations

The desired operating frequency is imposed into the system after comparing it with the frequency set from the power control loop. Then the angular frequency in rad/sec would be used to generate unity three phase balanced signal and they are used for the pulse's generation. The voltage transfer ratio q would multiply by these unity signals and this would decide the output voltage and input current. The Figure 6 shows generation of three phase-controlled reference signals [15], [18]–[23], [14], [24]–[33].

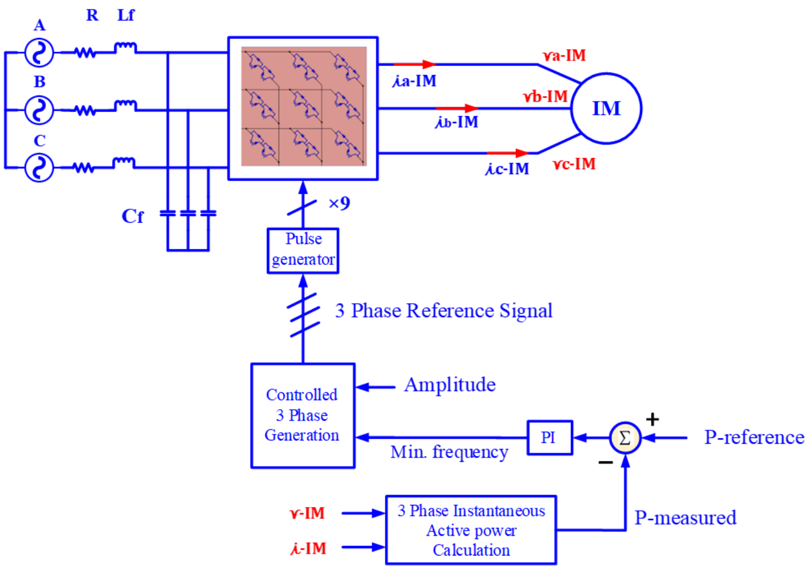

Figure 5. The power control loop of DMC

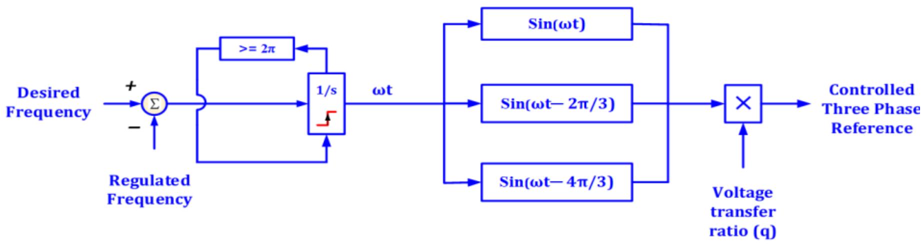

Figure 6. Reference signal generation

4. SIMULATION RESULTS AND DISCUSSION

The system is simulated under different conditions. The system parameters are listed in Table 2. The unity reference signals and angular frequency, and input and output voltage sector are shown in Figures 7(a) and 7(b) respectively. It is noticed that the angular frequency is locked with the reference signal which means perfect synchronization.

Table 2. System parameters

Parameter	Value
Grid voltage	380 V
Grid frequency	50 Hz
Input inductance filter	0.6 mH and 0.013 Ω
Input capacitance filter	900 μF
Switching frequency	4 kHz
Rated power	100 kW
Induction Generator rating	150 HP, 400 V, 50 Hz, 1487 rpm

The first scenario is when the system is tested to operate at different output frequencies with three-phase line to line 380 $V\ rms$ and 100 kW load. Firstly, the output voltage's amplitude and frequency are set to 0.85 and 50 Hz respectively. The grid voltage and current are shown in Figure 8 and they are in phase, which means unity power factor is achieved.

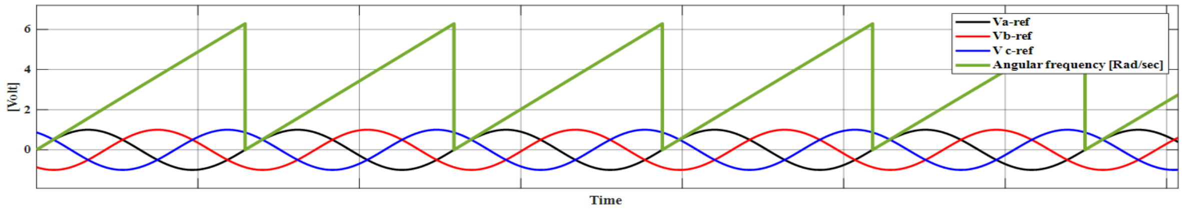

(a)

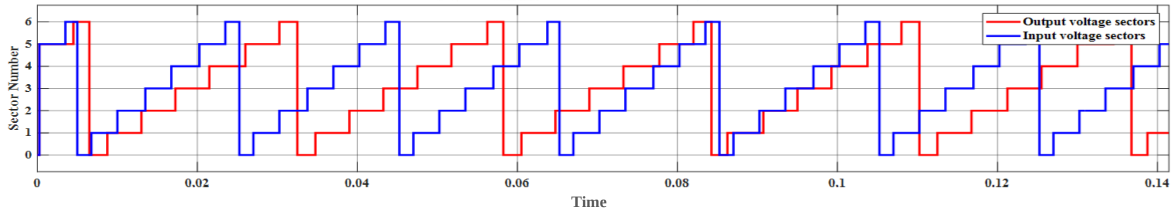

(b)

Figure 7. Result for reference signals and sector identification, (a) reference signals and angular frequency and (b) input voltage and load voltage sectors

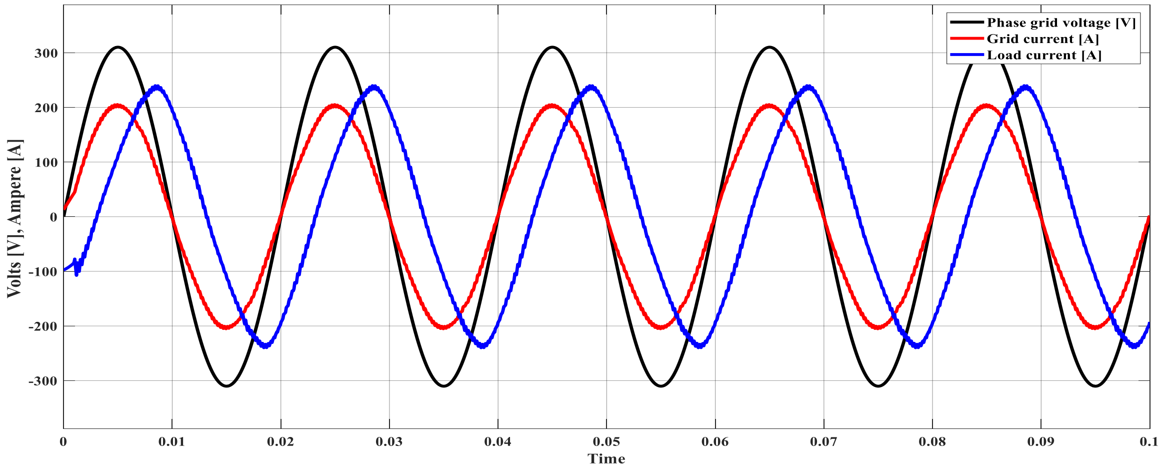

Figure 8. The DMC input voltage and current, and load current

The load current must be bigger than the input current, which would be noticed later. This might be explained by the fact that MC functions resemble to a buck (forward) converter in that it steps down the voltage and assumes that the system is 100% efficient with no energy storage components, thus the AC power that is supplied is equal to the output AC power. The output or load current exceeds the input current because the voltage transfer ratio q is smaller than unity, and this is demonstrated as (14) and (15):

$$P_{in} = P_{out} \tag{14}$$

$$V_{in} I_{in} \cos(\emptyset_{in}) = V_{out} I_{out} \cos(\emptyset_{out}) \tag{15}$$

Where, $\emptyset_{in}$ and $\emptyset_{out}$ are the input and output current displacement angles, respectively. The modulation has arranged such that $\cos(\emptyset_{in}) \cong 1$.

$$I_{in} = \frac{V_{out}}{V_{in}} I_{out} \cos(\emptyset_{out}) \tag{16}$$

The voltage transfer ratio $q = V_{out}/V_{in} < 1$ and $\cos(\emptyset_{out})$ is always less than unity therefore the input current is less than the load current I_{out}.

$$I_{in} = q \times I_{out} \cos(\emptyset_{out}) \tag{17}$$

The output voltage and averaged output voltage, and current at frequency 30 Hz and 100 Hz are shown respectively in Figures 9(a) and 9(b). Thus, it has assured that the MC could have output frequency less and over the supplied frequency. Figures 10 and 11 show the load voltage profiles at different output frequencies. Where Figure 10(a) and Figure 11(a) are load phase voltage with respect to the load neutral, Figure 10(b) and Figure 11(b) are load phase voltage with respect to the reference point of the source and Figure 10(c) and Figure 11(c) are the line-to-line output voltage. In Figures 10 and 11, the voltage transfer ratio is $q = 0.85$. Although these voltages have switching frequency pulses, but their averages produce a sinusoidal waveform. From Figures 10 and 11, the output phase voltages with respect to the neutral of the loads have sinusoidal waveforms with pulses at a frequency of 4 kHz.

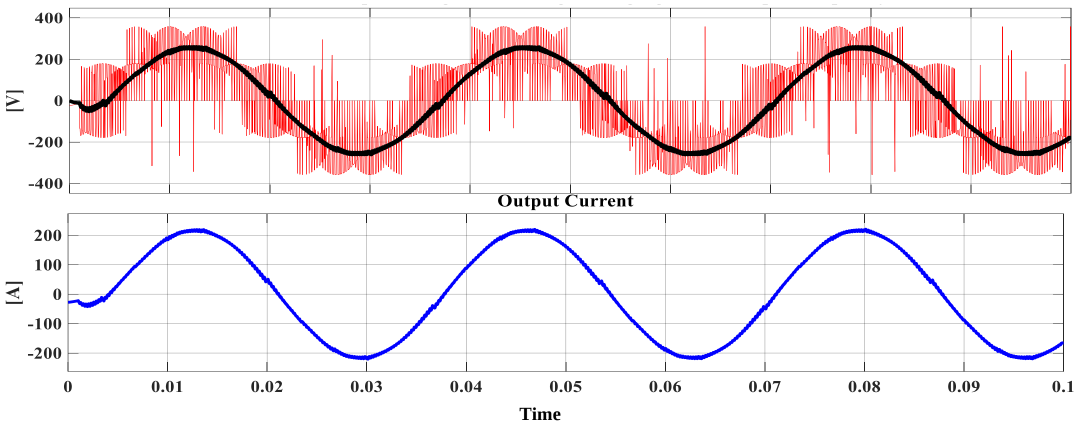

(a)

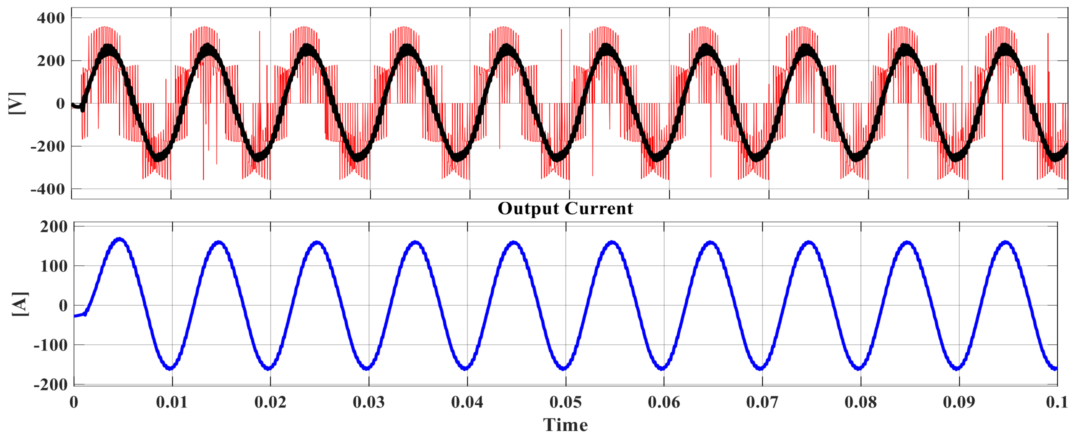

(b)

Figure 9. The DMC output phase voltage and current at (a) at 30 Hz and (b) at 100 Hz, output frequency

The second scenario is when the grid power is controlled. Induction generators (IGs) are modeled in the mode where an external signal controls the rotating speed. The controlled three-phase generation block shown in Figure 5 determines the IG operating frequency, and both the frequency and amplitude of the output signal can be adjusted.

In the simulation, the frequency is regulated by the PI power controller, while the amplitude is set to 0.85. At $t = 1\,s$ from the simulation time, its reference, which initially equals zero, changed to $-100\,kW$ while rising to 100 kW at $t = 2\,s$. The rotation frequency of the IG, which is 118 rad/s, rises to 120 rad/s at $t = 3\,s$. In Figure 12(a) speed, Figure 12(b) torque and Figure 12(c) (see Appendix) grid power are illustrated, where the IG speed, its torque, and the grid power are displayed. After the initial error, which could be due to the inertia of the IG, is minimized by the PI power controller, it can be seen that the reference power value is maintained despite both reference variation and perturbation (rotation speed changing).

One significant feature of MC is the grid current distortion. In Figure 13 (see Appendix), grid current without Figure 13(a) and with a harmonic filter are displayed. 5th harmonic filter is used, where filter

VA rating would have an impact of the grid current THD as shown in Figures 13(b) and 13(c). The THD is reduced from 6.41 % to 2.31 %.

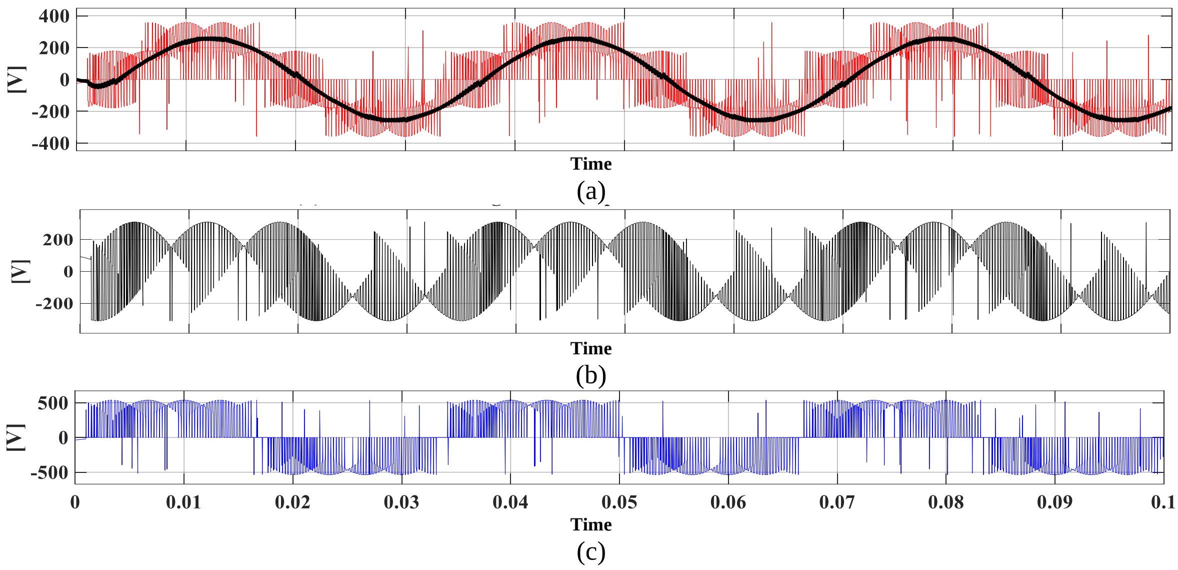

Figure 10. Responses of load voltage profile at 30 Hz (a) load phase voltage with respect to the load neutral, (b) load phase voltage with respect to the reference point of the source, and (c) output line to line voltage and at 30 Hz output frequency

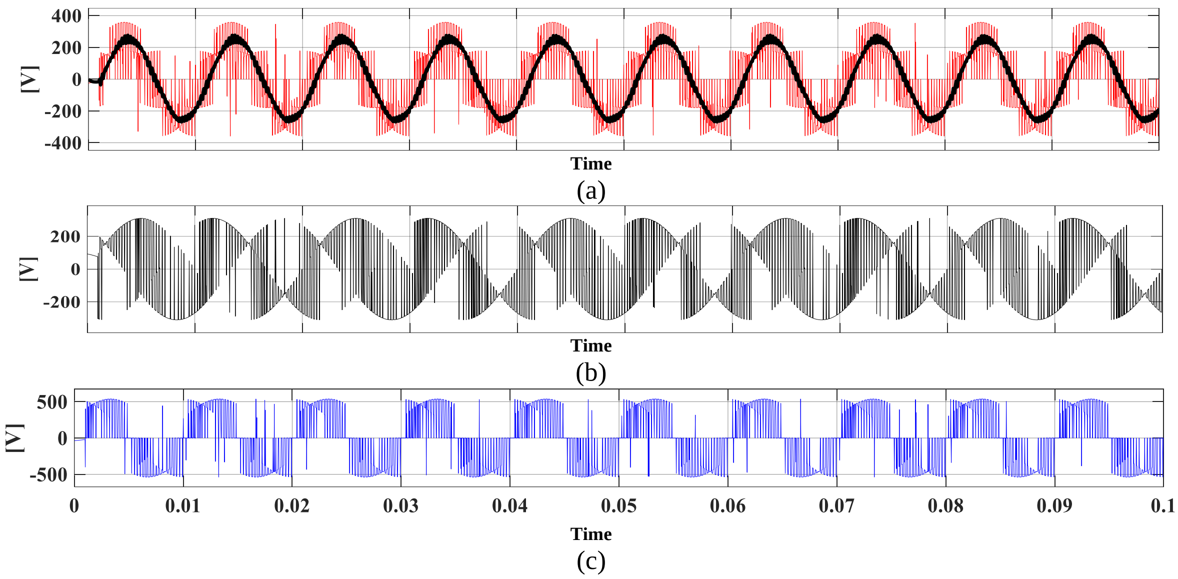

Figure 11. Responses of load voltage profile at 100 Hz (a) load phase voltage with respect to the load neutral, (b) load phase voltage with respect to the reference point of the source, and (c) output line to line voltage at 100 Hz output frequency

5. CONCLUSION

Single stage AC/AC direct matrix converter is operated by space vector modulation directly and it has shown that the input power factor can be changed in addition to the ability to generate input and output sine currents with various frequencies. That would make the matrix converter suitable for variable frequency drive applications. Because double-side modulation improves the harmonic performance of the MC input and output sides at the cost of only slightly increasing the number of branch-switch-overs (BSO) each switching period, it has been employed instead of single-side modulation. The grid power is controlled by implementing a simple power control loop that would generate a three-phase controlled reference signal for pulses generation. The DMC simulation results show that the input current is maintained in a sinusoidal shape and the output current could have a frequency less or above the input frequency. The grid power is controlled and it is stable regardless of the variation of IG speed.

APPENDIX

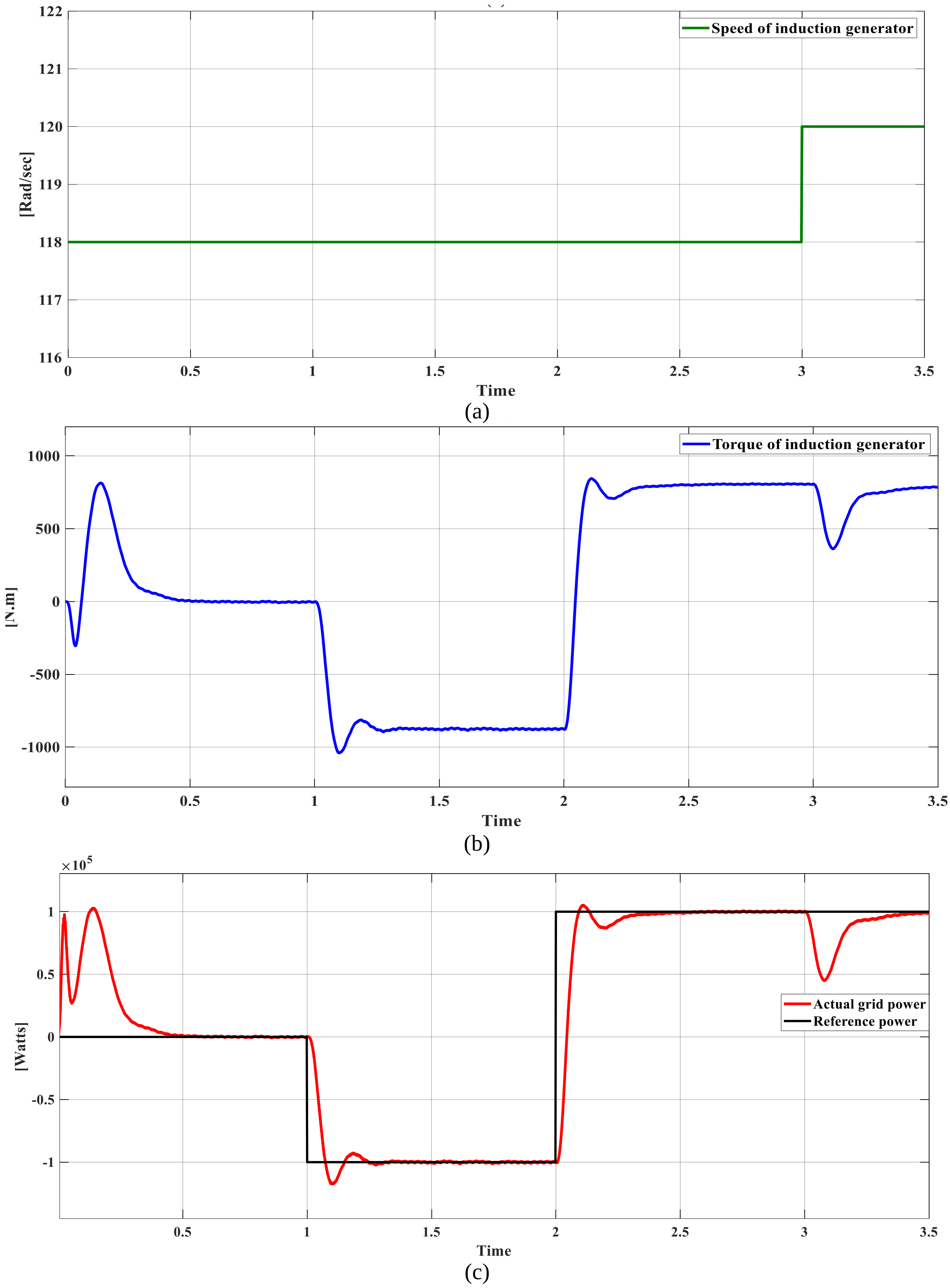

Figure 12. The speed: (a) torque, (b) grid power, and (c) of DMC

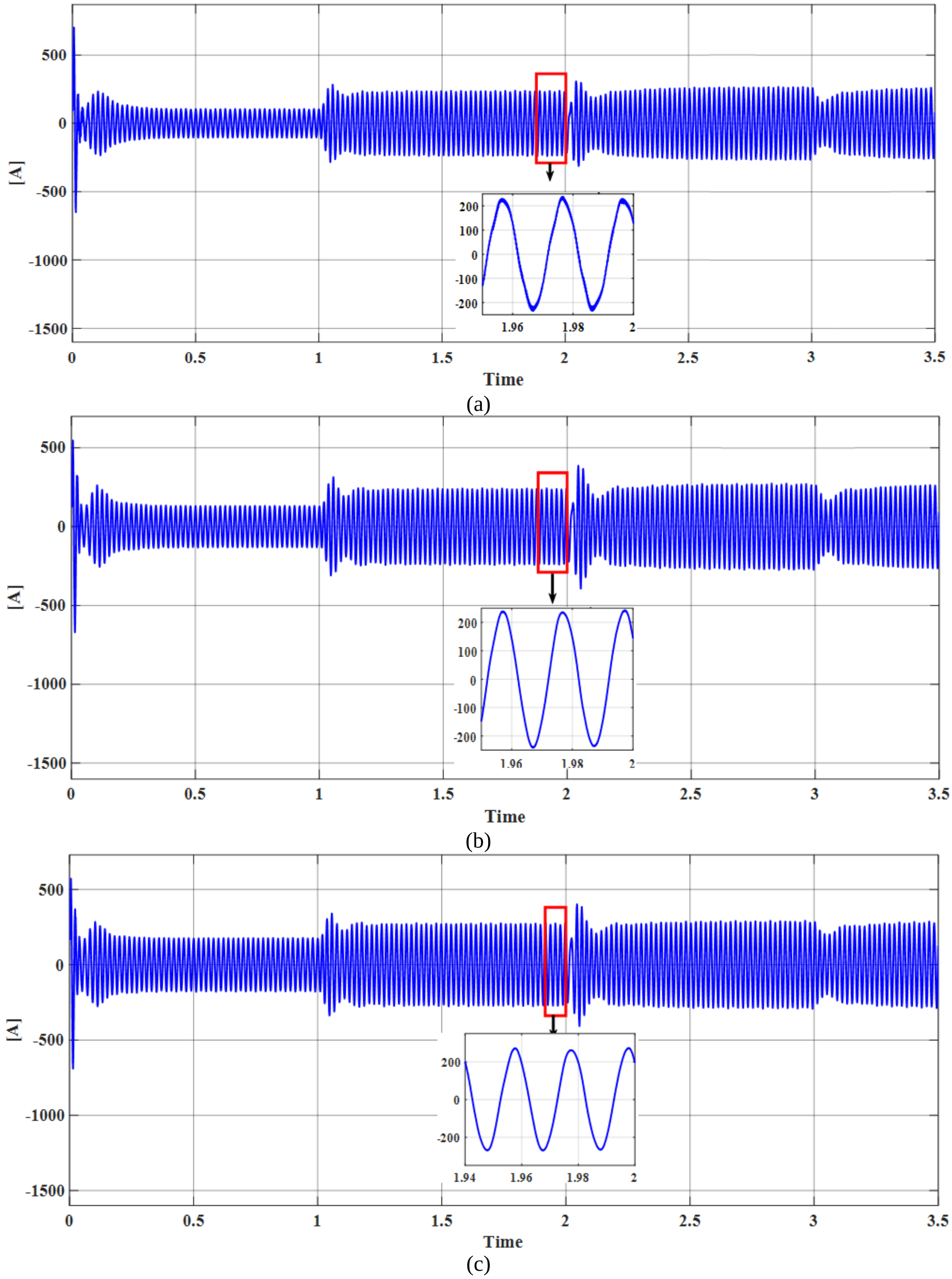

Figure 13. The grid current: (a) without filter THD= 6.41%, (b) with 10 KVA filter THD 4.59%, and (c) with 30 KVA filter THD 2.31%

REFERENCES

[1] R. W. Erickson, "Converter Circuits," *Fundamentals of Power Electronics*, pp. 135–190, 1997, doi: 10.1007/978-1-4615-7646-4_6.

[2] P. W. Wheeler, J. Rodríguez, J. C. Clare, L. Empringham, and A. Weinstein, "Matrix converters: A technology review," *IEEE Transactions on Industrial Electronics*, vol. 49, no. 2, pp. 276–288, 2002, doi: 10.1109/41.993260.

[3] D. Varajão and R. E. Araújo, "Modulation methods for direct and indirect matrix converters: A review," *Electronics (Switzerland)*, vol. 10, no. 7, 2021, doi: 10.3390/electronics10070812.

[4] J. Rodriguez, M. Rivera, J. W. Kolar, and P. W. Wheeler, "A review of control and modulation methods for matrix converters," *IEEE Transactions on Industrial Electronics*, vol. 59, no. 1, pp. 58–70, 2012, doi: 10.1109/TIE.2011.2165310.

[5] S. H. Hosseini and E. Babaei, "A new generalized direct matrix converter," *IEEE International Symposium on Industrial Electronics,* vol. 2, pp. 1071–1076, 2001, doi: 10.1109/isie.2001.931624.

[6] Z. Malekjamshidi, M. Jafari, and J. Zhu, "Analysis and comparison of direct matrix converters controlled by space vector and Venturini modulations," in *2015 IEEE 11th International Conference on Power Electronics and Drive Systems*, Jun. 2015, pp. 635–639. doi: 10.1109/PEDS.2015.7203550.

[7] P. Resutik, S. Kascak, and J. Kellner, "Design, Simulation, and Analysis of Compact 3x1 Matrix Module Prototype in 3x3 Matrix Converter Application," *14th International Conference ELEKTRO, ELEKTRO 2022 - Proceedings*, 2022, doi: 10.1109/ELEKTRO53996.2022.9803766.

[8] D. Anbazhagan and K. Govindarajan, "Direct Space Vector Modulated Matrix Converter and its Dynamic Model Study," 2012, [Online]. Available: https://www.researchgate.net/publication/304407560

[9] R. Ghoni, A. N. Abdalla, S. P. Koh, H. F. Rashag, and R. Razali, "Issues of matrix converters: Technical review," *International Journal of Physical Sciences*, vol. 6, no. 15, pp. 3628–3640, 2011, doi: 10.5897/IJPS11.271.

[10] K. Omrani, M. A. Dami, and M. Jemli, "A SVM control strategy for a direct matrix converter," *International Conference on Green Energy and Conversion Systems, GECS 2017*, no. 3, 2017, doi: 10.1109/GECS.2017.8066130.

[11] P. Kiatsookkanatorn and S. Sangwongwanich, "A Unified PWM Strategy to Reduce Minimum Switching Number for Matrix Converters," *2022 International Power Electronics Conference, IPEC-Himeji 2022-ECCE Asia*, no. 2, pp. 83–88, 2022, doi: 10.23919/IPEC-Himeji2022-ECCE53331.2022.9807207.

[12] A. El Aroudi, E. Rodriguez, and M. Orabi, "Modeling of switching frequency instabilities in buck- based DC – AC H-bridge inverters," *International Journal of Circuit Theory and Applications*, 2010, doi: 10.1002/cta.

[13] Y. Han, B. Han, X. Ni, P. Qiu, and Z. Xiang, "Research on grounding mode of AC-AC converter system," pp. 1302–1306, 2022, doi: 10.1049/icp.2022.1403.

[14] A. Benachour, E. Berkouk, and M. O. Mahmoudi, "Study and implementation of indirect space vector modulation (ISVM) for direct matrix converter," *3rd International Conference on Control, Engineering and Information Technology, CEIT 2015*, pp. 2–7, 2015, doi: 10.1109/CEIT.2015.7233039.

[15] J. M. Lozano-Garcia and J. M. Ramirez, "Voltage compensator based on a direct matrix converter without energy storage," *IET Power Electronics*, vol. 8, no. 3, pp. 321–332, 2015, doi: 10.1049/iet-pel.2014.0099.

[16] P. Patel and M. A. Mulla, "Space vector modulated three-phase to three-phase direct matrix converter," *EEEIC 2016 - International Conference on Environment and Electrical Engineering*, no. Imc, 2016, doi: 10.1109/EEEIC.2016.7555820.

[17] M. Mihret, "Modeling, stability analysis and control of a direct AC/AC matrix converter based systems," 2012.

[18] A. J. L. Helle, K. Larsen, *Design and Control of Matrix Converters*. 2004. doi: 10.1007/978-981-10-3831-0.

[19] S. Orcioni, G. Biagetti, P. Crippa, and L. Falaschetti, "A driving technique for AC-ac direct matrix converters based on sigma-delta modulation," *Energies*, vol. 12, no. 6, pp. 1–18, 2019, doi: 10.3390/en12061103.

[20] M. A. Perez, C. A. Rojas, J. Rodriguez, and H. Abu-Rub, "A simple modulation scheme for a three-phase direct matrix converter," *IEEE International Symposium on Industrial Electronics*, pp. 105–110, 2012, doi: 10.1109/ISIE.2012.6237067.

[21] Z. Malekjamshidi, M. Jafari, D. Xiao, and J. Zhu, "Analysis of direct matrix converter operation under various switching patterns," *Proceedings of the International Conference on Power Electronics and Drive Systems*, vol. 2015-August, pp. 630–634, 2015, doi: 10.1109/PEDS.2015.7203549.

[22] A. K. Singh and A. K. Singh, "Implementation of Direct Matrix Converter using hybrid modulation with minimized losses," *IECON Proceedings (Industrial Electronics Conference)*, pp. 846–851, 2013, doi: 10.1109/IECON.2013.6699244.

[23] S. Ansari and A. Chandel, "Simulation based comprehensive analysis of direct and indirect matrix converter fed asynchronous motor drive," *2017 4th IEEE Uttar Pradesh Section International Conference on Electrical, Computer and Electronics, UPCON 2017*, vol. 2018-Janua, pp. 9–15, 2017, doi: 10.1109/UPCON.2017.8251014.

[24] L. Ming *et al.*, "A SiC-Si Hybrid Module for Direct Matrix Converter With Mitigated Current Spikes," *IEEE Journal of Emerging and Selected Topics in Power Electronics*, vol. 10, no. 4, pp. 3805–3817, 2022, doi: 10.1109/JESTPE.2021.3093627.

[25] J. Igney and I. Hahn, "Modulation Strategy and Control Range Function for Matrix Converters Without Trigonometric Functions," *2022 International Symposium on Power Electronics, Electrical Drives, Automation and Motion, SPEEDAM 2022*, pp. 553–560, 2022, doi: 10.1109/SPEEDAM53979.2022.9842119.

[26] A. Dasgupta and P. Sensarma, "An integrated filter and controller design for direct matrix converter," *IEEE Energy Conversion Congress and Exposition: Energy Conversion Innovation for a Clean Energy Future, ECCE 2011, Proceedings*, no. May 2014, pp. 814–821, 2011, doi: 10.1109/ECCE.2011.6063854.

[27] M. Leubner, N. Remus, M. Stübig, and W. Hofmann, "Active stabilization of direct matrix converter input side filter through grid current control," *Conference Proceedings - IEEE Applied Power Electronics Conference and Exposition - APEC*, vol. 2016-May, no. 2, pp. 2175–2181, 2016, doi: 10.1109/APEC.2016.7468168.

[28] E. Purwanto, F. D. Murdianto, D. Wahyu Herlambang, G. Basuki, and M. P. Jati, "Three-phase direct matrix converter with space vector modulation for induction motor drive," *Proceedings of ICAITI 2019 - 2nd International Conference on Applied Information Technology and Innovation: Exploring the Future Technology of Applied Information Technology and Innovation*, pp. 11–16, 2019, doi: 10.1109/ICAITI48442.2019.8982139.

[29] A. Babaei and W. Ziomek, "The Improvement of Power Quality in an ac-ac Direct Matrix Converter by Using Hybrid Filters," no. July, pp. 20–22, 2022.

[30] L. R. Merchan, J. M. L. Garcia, A. Pizano-Martinez, E. A. Zamora-Cardenas, H. J. Estrada-Garcia, and L. C. Razo-Vargas, "Output filter control for matrix converter in synchronous applications," *2016 IEEE International Autumn Meeting on Power, Electronics and Computing, ROPEC 2016*, no. November, 2017, doi: 10.1109/ROPEC.2016.7830577.

[31] B. Babes, O. Aissa, N. Hamouda, and I. Colak, "Model Based Predictive Direct Torque and Flux Control for Grid Synchronization of a PMSG Driven by a Direct Matrix Converter," pp. 208–213, 2022, doi: 10.1109/icsmartgrid55722.2022.9848534.

[32] C. Gili, G. D. Lozano, A. Péres, and S. V. G. Oliveira, "Experimental study of a direct matrix converter driving an induction machine," *COBEP 2011 - 11th Brazilian Power Electronics Conference*, pp. 232–237, 2011, doi: 10.1109/COBEP.2011.6085321.

[33] E. M. Khalil, N. Mohamed, H. Mohamed, and S. Lassad, "Enhancement of Finite Set Model Predictive Control for Direct Matrix Converter fed DFIG-Wind Energy Conversion System," *ENERGYCON 2022 - 2022 IEEE 7th International Energy Conference, Proceedings*, no. Energycon, pp. 5–10, 2022, doi: 10.1109/ENERGYCON53164.2022.9830152.

BIOGRAPHIES OF AUTHORS

Ali Salam Kadhim Al-Khayyat received the B.Sc. degree in Electrical Engineering from Al-Kufa University/Iraq in 2008, and the M.Sc. degree in Electrical Engineering for Sustainable and Renewable Energy System from Nottingham University, UK in 2014. He joined the faculty of Engineering in University of Thi-Qar since 2016. He is currently Assistant Professor at the department of Electrical and Electronics Engineering Department in University of Thi-Qar. His research interests are power electronics converter control, power quality and renewable energy. He can be contacted at email: ali-al-khayyat@utq.edu.iq.

Humam Qahtan Kadhem received the B.Sc. and M.Sc. degree in Electrical Power Engineering from Al-Basrah University. He is currently assistant lecturer at Southern Technical University -Iraq. His research interests are power system, machines and control systems engineering. He can be contacted at email: humam.alhasan@stu.edu.iq.

Mustafa Jameel Hameed received the B.Sc. degree in Electrical Power Engineering from Al-Furat Al-Awsat Technical University/ Iraq in 2011, and the M.Sc. degree in Electrical Engineering for Electrical power systems and networks from South Russian State Technical University/ RU in 2015. He joined the faculty of Engineering in University of Thi-Qar since 2016. He is currently lecturer at the department of Electrical and Electronics Engineering Department in University of Thi-Qar. His research interests are power generation and transmission, power electronic control, power quality and renewable energy. He can be contacted at email: mustafa-j@utq.edu.iq.